Structure-Guided Generation of a Redox-Independent Blue Fluorescent Protein from mBFP

Pil-Won Seo[1,†], Eun-Seo Jo[2,†], Sung-Hwan You[2], Dae-Eun Cheong[2], Geun-Joong Kim[2] and Jeong-Sun Kim[1]

*1 - **Department of Chemistry,** Chonnam National University, Gwangju 61186, Republic of Korea*
*2 - **Department of Biological Sciences,** Chonnam National University, Gwangju 61186, Republic of Korea*

***Correspondence to Geun-Joong Kim and Jeong-Sun Kim:**. gjkim@chonnam.ac.kr, jsunkim@chonnam.ac.kr.*
https://doi.org/10.1016/j.jmb.2019.06.005
Edited by Bert Poolman

Abstract

Fluorescent proteins, such as the green fluorescent protein, are used for detection of cellular components and events. However, green fluorescent protein and its derivatives have limited usage under anaerobic conditions and require a long maturation time. On the other hand, the NADPH-dependent blue fluorescent protein (BFP) without oxidative modification of residues is instantly functional in both aerobic and anaerobic systems. BFP proteins belong to a short-chain dehydrogenase/reductase (SDR) protein family, and their fluorescent property changes with reaction time in the presence of a substrate. With the aim of developing a better fluorescent reporter independent of redox state, we elucidated the crystal structure of a tetrameric mBFP from soil metagenomes with and without NADPH. Apart from the previously known regions, structure-guided mutational studies have identified several residues that contribute to the fluorescence of mBFP, including two aromatic residues (F97 and Y157) near the nicotinamide moiety of the bound NADPH. A single histidine mutation at Y157 (Y157H) has conferred more stabilized, time-independent fluorescence even in the presence of substrates. Furthermore, we discovered another SDR protein that can also emit blue fluorescence. These results open a new possibility for the development of BFP as a stable cellular reporter for widespread use, independent of subcellular environments.

Introduction

Fluorescent proteins with inherent fluorophores are widely used for the detection of intracellular locations of macromolecules or for determining the abundance of metabolites in organelles [1–3]. The discovery of the green fluorescent protein in jellyfish *Aequorea victoria* has had great influence on cellular detection and imaging, and several green fluorescent protein (GFP) derivatives with different fluorescent excitation/emission spectra from their parent protein have been developed [4,5]. However, GFP and its derived proteins require strictly aerobic conditions, since their critical chromophore is formed by oxidative remodeling of the existing amino acids at a specific site after biosynthesis [6,7]. This requisite chemical transition restricts their usage as an imaging probe and/or reporter in anaerobic conditions. In addition, these fluorescent proteins require a rather long maturation time for their maximal fluorescence *in vivo*, which might pose an obstacle for real time detection and monitoring of cellular events. These shortcomings with GFPs suggest a necessity to develop oxygen-independent fluorescence proteins with a short maturation time [8–12], especially *in vivo* real time detection of NADPH-dependent cellular events under the oxygen-limited conditions.

Interestingly, several cellular proteins can become fluorogenic upon interaction with a cofactor such as nicotinamide adenine dinucleotide phosphate (NADPH) and flavin mononucleotide (FMN) [13–15]. In contrast to GFPs, the cofactor-dependent fluorescence is readily detectable since the fluorescent capacity is instantaneously formed upon binding a cofactor, without requiring large structural changes in either the protein or the bound cofactor. Although a cofactor is necessary for

fluorescence, the co-expression of a cofactor with the cofactor-dependent fluorescent protein is not always required, since they can uptake the regenerated cofactors from the cellular environment. Nevertheless, not all of the cofactor-binding proteins are able to emit detectable fluorescence. NADPH- and FAD-dependent fluorescent systems basically share a working principle that well function as cofactors in a dependent manner under anaerobic condition, but direct comparison study between two systems is not conducted up to date. Recent reports revealed the existence of some proteins that are fluorescent in the presence of NADPH [13,16], called NADPH-dependent blue fluorescent proteins (BFPs). Especially, fluorescence was measured in the anaerobic condition and recorded soon (within 1 min) after the addition of NADPH into the solution containing the isolated BFP protein from the soil metagenomic library (metagenome-derived BFP, or mBFP) [13]. When compared to the typical fluorescent proteins GFPuv (a variant of green fluorescent protein, F99S/M153 T/V163A) and DsRed (a red fluorescent protein from *Discosoma* sp), mBFP showed a distinct blue fluorescence under the strict anaerobic condition, having a promising potential for the practical use as a reporter in a specific condition. Sequence analysis has shown that BFPs belong to a short-chain dehydrogenase/reductase (SDR) family that oxidizes or reduces cellular substances including various aldehydes [16], and indicate the oxidation level of bound NADPH with the proportional decrease of their fluorescence. Thus, the enzymatic property of BFPs can limit their performance as a stable reporter protein in the cytosolic condition in the presence of potential substrates. However, if their dehydrogenase and/or reductase activity is inhibited by blocking substrate access to their active sites, or removed by inducing structural deformation with no catalytic activity, then these BFPs can be employed as powerful reporter proteins.

In our previous report, we identified the blue fluorescent capacity of mBFP to be comparable to another BFP from *Vibrio vulnificus* (BFPvv) [13]. The optimized condition and affecting parameters for the detection of fluorescence signal of mBFP and NADPH complex were recently reported [17]. Although sequence homology between the two BFPs is not significant (~20%), the sequence analysis classifies them as part of the SDR family proteins. Furthermore, biochemical assays showed that mBFP can reduce nitrobenzaldehyde in the presence of NADPH by catalytic activity. In this study, we elucidated the crystal structures of mBFP with and without NADPH. Furthermore, we analyzed residues that influence the fluorescence of the mBFP–NADPH complex at the probable substrate-binding site. Structure-guided mutagenesis confirmed the residues' role in the fluorescent capacity of mBFP. We isolated an mBFP derivative that exhibits stable fluorescence in the presence of putative substrates under various analytical conditions. Moreover, we identified another SDR family protein (PDB ID 5u2w) from *Burkholderia cenocepacia* J2315 (BFPbc) with blue fluorescent capacity in the presence of NADPH, which is comparable to mBFP and BFPvv. In summary, our results will provide a foundation for the platform technology of stable and real-time detection of NADPH *in vitro* and *in vivo*.

Results and Discussion

Overall structural features of mBFP

The recombinant mBFP was homogeneously purified to ≫99% purity using sequential chromatographic methods, and its oligomeric state in solution was analyzed using size-exclusion chromatography (SEC). Analysis of the SEC elution profile of recombinant mBFP and comparison with that of the referenced proteins (Supplementary Fig. 1) suggests that mBFP in solution migrates in tetrameric form, as predicted by a previous report [13].

The crystal structure of mBFP was solved by the molecular replacement method using a short-chain dehydrogenase from *Sinorhizobium meliloti* 1021 (PDB ID 3V2G) as the search model. The structure was refined to a resolution of 2.3 Å (Table 1). The asymmetric unit has four protein molecules that form a tetrameric structure stabilized by a large hydrophobic interface among nearby molecules (Fig. 1a). The monomeric protein has a central seven-stranded β-sheet flanked with several α-helices at both sides (Fig. 1b). The conformations of individual monomers in the tetrameric mBFP structure are in good agreement, and all monomers superimpose (Fig. 1b) with rmsd values of less than 0.35 Å. At the dimeric interface, the two α-helices (α4 and α5) form a four-helical bundle together with two α-helices of a neighboring molecule. In the tetrameric structure of mBFP, two dimers further assemble in opposite directions, as the β7-strand of the central β-sheet of one dimer contacts that of the neighboring protomer in a parallel manner (Fig. 1).

NADPH binding site

The mBFP–NADPH crystal structure was directly refined using the diffraction data collected from the single crystal soaked into the precipitant solution containing 6.7 mM NADPH. The bound NADPH is located in the surface pocket of each protomer, which is formed by the central globular fold and the protruding α-helix on the top (Fig. 1b). In the tetrameric structure, the NADPH-binding sites of the two diagonal molecules face the same side, while those of the neighboring two molecules are on the opposite side.

Table 1. Data collection and structure refinement statistics

Data collection	apo-mBFP	NADPH-mBFP
Space group	$P2_12_12_1$	$P2_12_12_1$
Unit cell dimensions		
a, *b*, *c* (Å)	56.28, 90.56, 171.53	54.66, 96.79, 168.94
α, *β*, *γ* (°)	90, 90, 90	90, 90, 90
Wavelength (Å)	0.9794	0.9793
Resolution (Å)	50–2.3 (2.34–2.30)[a]	20-2.3 (2.34–2.30)[a]
R_{sym}	20.4 (74.9)	18.3 (77.7)
R_{pim}	8.8 (32.7)	7.0 (29.6)
$I/\sigma(I)$	17.8 (3.6)	8.5 (1.7)
Completeness (%)	99.8 (99.7)	99.5 (99.8)
Redundancy	6.2 (6.1)	7.4 (7.5)
Refinement		
No. of reflections	39,065	40,137
R_{work}/R_{free}	20.5 (19.8)/25.6 (27.7)	23.6 (28.9)/26.2 (34.5)
No. atoms		
Protein/water/ligand	7091/273	7100/240/192
Bond lengths (Å)/angles (°)	0.006 / 0.87	0.003 / 0.88
Average *B*-values (Å^2)		
Protein/water/ligand	35.7/36.9/0	31.6/30.0/42.2
Ramachandran plot (%)		
Favored/allowed/outliers	98.6/1.4/0.0	98.1/1.9/0.0
PDB ID	6J7H	6J7U

[a] The numbers in parentheses are the statistics from the highest-resolution shell.

As NADPH binds to mBFP, it introduces a structural change of the protein in two regions: one region (G188–R201) between the β6-strand and the α6-helix (β6–α6 loop) that contacts the nicotinamide ring moiety and the other at another loop (β2–α2 loop) around the phosphate-contacting region at the adenine nucleotide moiety (Fig. 1c). NADPH binding reorients the β6–α6 loop toward the carboxamide moiety of the bound NADPH, where the side-chain hydroxyl group of T192 interacts with the amide group and the side-chain atom of N194 hydrogen-bonds with the amide and carbonyl groups of the bound NADPH (Fig. 1d). Some of the main-chain atoms (P187–T192) in this β6–α6 loop further form hydrogen bonds with the carbonyl moiety of the nicotinamide ring. Upon binding to NADPH, the β2–α2 loop of mBFP contacts the phosphate group at the 2′-OH of the ribose sugar moiety in the adenine nucleotide (Fig. 1d).

The ribose sugar ring moiety of the nicotinamide nucleotide of the bound NADPH is also involved in interaction with mBFP by forming a hydrogen bond with the Y157 hydroxyl group on the α5-helix. This Tyr residue is located ~3.5 Å from the nicotine ring and makes a T-shape aromatic interaction with the F97 on the surface (Fig. 1d).

mBFP shares a conserved fold with short-chain alcohol dehydrogenases/reductases

The structural features of the mBFP protein are conserved in other SDR family proteins, and their quaternary structures are well superimposed (Fig. 2a), with low rmsd values. Both the NADPH-binding site and the residues forming the tetrameric assembly in other SDR proteins are conserved in the mBFP of this study. The most significant difference in the superimposed structures of homologous proteins is found in the region near the nicotinamide ring moiety of NADPH-binding site (Fig. 2a and Supplementary Fig. 2). Whereas the compared SDR proteins have an elongated structure, only the BFPvv protein contains additional residues that form a helix–turn–helix motif and cover the nicotinamide moiety of the bound NADPH [14], resulting in the partially hidden NADPH bound to BFPvv (Fig. 2). In contrast, the nicotinamide ring of the bound NADPH to other SDRs, including mBFP, is exposed to the solvent surface.

Sequence comparison shows some extra residues between the β6-strand and the α6-helix in BFPvv (Supplementary Fig. 2), compared with mBFP and another SDR family protein from *B. cenocepacia* J2315 (PDB ID 5U2W, hereafter referred to as BFPbc). These residues are disordered in the three subunits of the tetrameric BFPvv, but a helix–turn–helix motif is formed at the corresponding region in the fourth subunit, which partially covers the fluorescent nicotinamide moiety of the bound NADPH [14] as shown in Fig. 2a. In order to examine the contribution of these residues to the fluorescence in BFPvv, we constructed a mutant with a short loop of a sequence extracted from mBFP. However, this BFPvv mutant exhibited a fluorogenic property similar to the wild-type protein (data not shown),

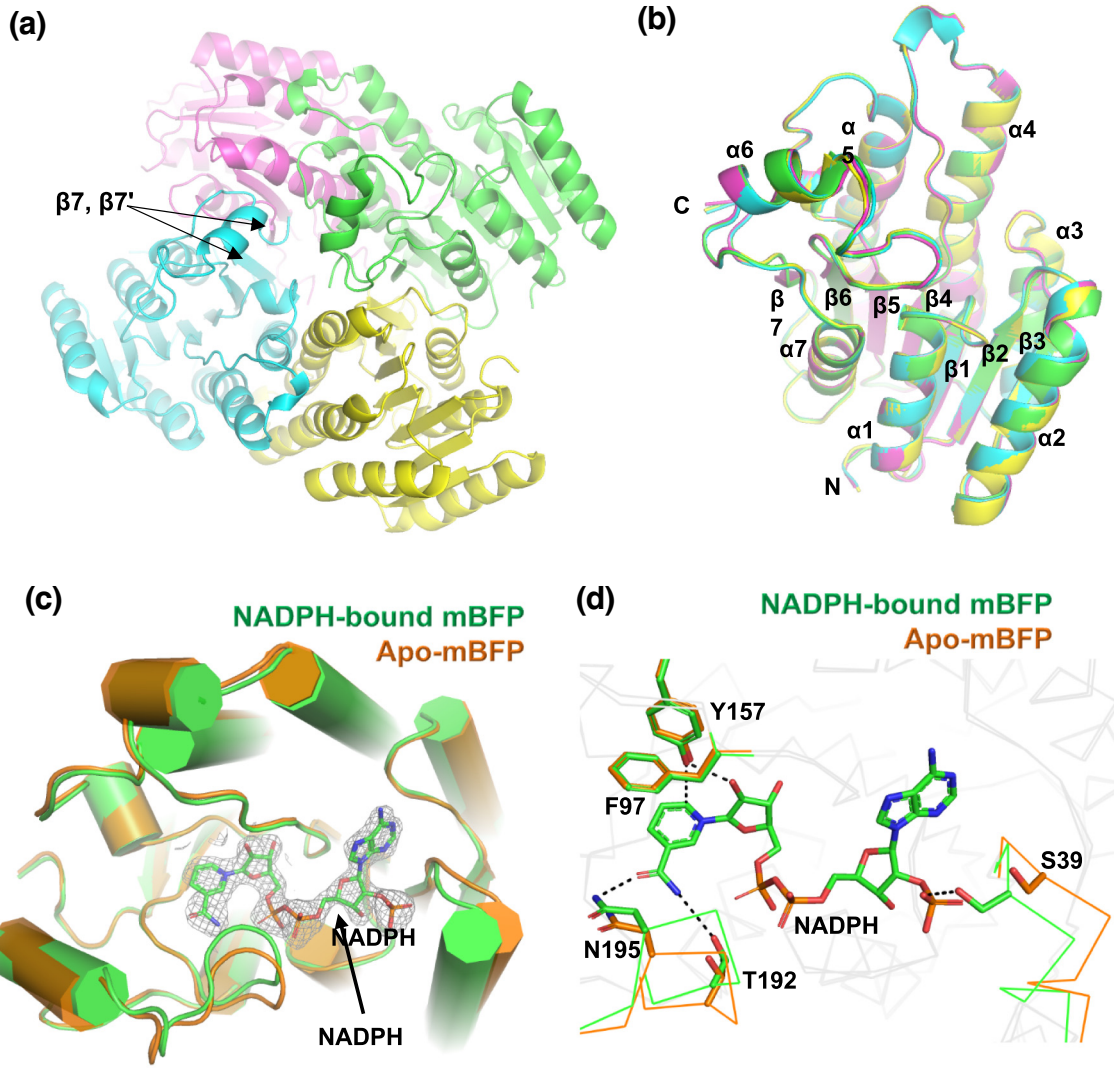

Fig. 1. Crystal structure of apo-mBFP and NADPH-bound mBFP. (a) Ribbon diagram of the tetrameric mBFP. The four mBFP molecules in the apo-structure are differentiated by color. (b) Four superimposed subunits of the tetrameric mBFP. (c) Superposition of apo-mBFP and NADPH-bound mBFP. The two structures were differentiated with colors, and the bound NADPH was depicted with a stick model in the $2F_o - F_c$ map contoured at 1.0σ level. A ribbon diagram showing α-helix (red), β-sheet (yellow), and loop (green) of mBFP with secondary-structure nomenclature. (d) Close-up view of the NADPH-binding site of mBFP. NADPH and the important residues for binding NADPH are represented as stick models.

indicating that the difference induced here does not affect the fluorescent capacity of BFPvv.

Since the two BFP proteins are closely related to the SDR family with regard to their sequences, and since they exhibit high similarity in their quaternary structures, we surmised that SDR proteins with a similar number of residues and quaternary structures in complex with NADP(H) might have an NADPH-dependent blue fluorescence. Based on the structural similarity search using the DALI server (http://ekhidna2.biocenter.helsinki.fi/dali/), we selected a short-chain dehydrogenase from *B. cenocepacia* J2315 (BFPbc), which is one of the best structural homologs of mBFP. We synthesized a sequence coding for this gene and expressed the protein in *Escherichia coli*. The purified recombinant BFPbc protein emitted a blue fluorescence, comparable to mBFP and BFPvv (Fig. 3). This result strongly implies that there is a high possibility that NADP(H)-dependent SDRs form BFPs.

Two aromatic residues are involved in mBFP fluorescence

The fluorescent capacity of mBFP is closely related to the electron distribution on the nicotinamide ring of NADPH. Hence, protein residues that directly or indirectly interact with the nicotinamide

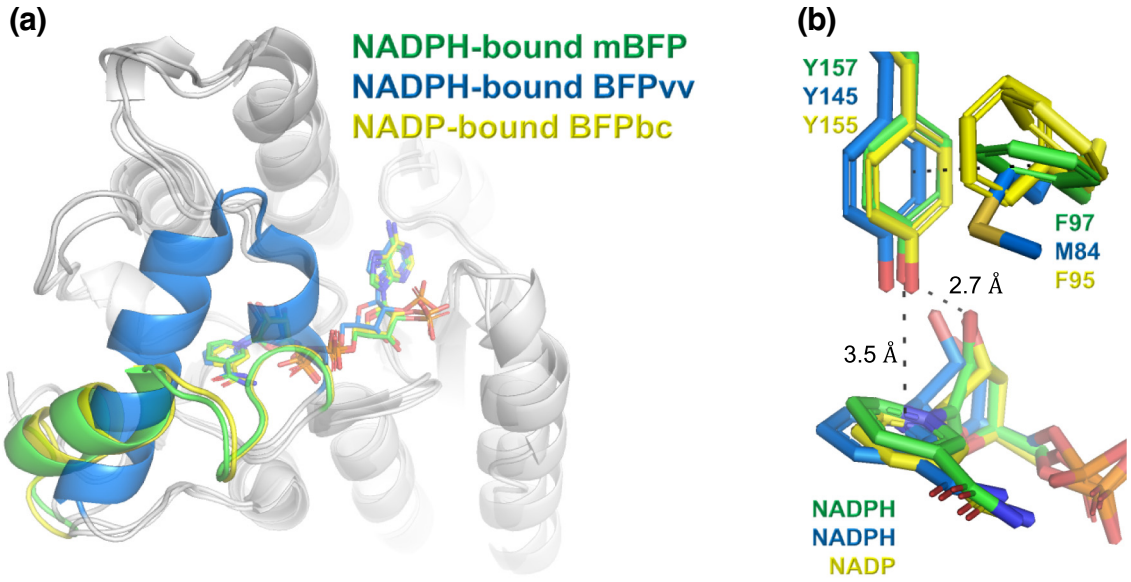

Fig. 2. Structural comparison of NADPH-bound mBFP, NADPH-bound BFPvv, and NADP-bound BFPbc. (a) Monomeric NADPH-bound mBFP, NADPH-bound BFPvv, and NADP-bound BFPbc are depicted by alternating colors. (b) Residues at the NADPH binding site, bound NADPH (mBFP, BFPvv), and NADP (BFPbc) are displayed as stick models.

moiety are capable of changing the electron distribution of nicotinamide ring of NADPH and thus influence the fluorescent property of mBFP. As described above, two protein regions interact with bound NADPH (Fig. 1d). The carboxamide moiety of nicotinamide directly interacts with residues of T192–G199 in the β6–α6 loop through a few hydrogen bonds. As expected, the introduced Ala mutation at N195 (N195A) exhibits decreased fluorescence of the protein (Fig. 3).

At the opposite site of the β6–α6 loop, the ribose sugar ring of the nicotinamide nucleotide moiety of NADPH directly interacts with the hydroxyl group of the Y157 side-chain (Figs. 1d and 2b). This residue further forms a T-shape aromatic interaction with F97. Y157 mutations with smaller residues of Leu, Asn, Val, and Ser decreased their protein's respective fluorescent properties (Fig. 3). However, its replacement with bulky side-chain residues has yielded conflicting results: incorporation of a His residue increased the protein's fluorescence, whereas a Trp residue decreased the fluorescence (Fig. 3). Among the compared BFP proteins, BFPvv, mBFP, and BFPbc (Supplementary Fig. 2), the first aromatic residue (Y157 of mBFP) is well conserved, unlike the second aromatic residue (F97 of mBFP). A decreased fluorescent property was observed when small residues (F97A, F97S, and F97G) or large hydrophilic residues (His, Lys, and Asn) are replaced at the corresponding site (Fig. 3). On the other hand, replacement with a Met residue exhibited fluorescence comparable to the wild-type (Fig. 3), indicating that hydrophobic masking at this position affects the fluorescence of mBFP.

In summary, structure-guided mutational studies have demonstrated that the aromatic residue affects the fluorescence of the mBFP protein by hydrogen-bonding with the ribose sugar of the nicotinamide nucleotide of the bound NADPH and its nearby hydrophobic Phe residue.

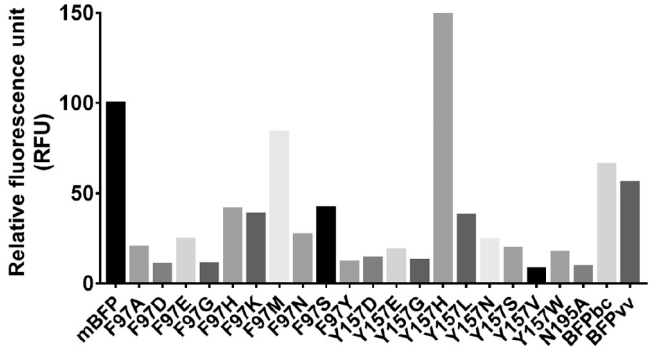

Fig. 3. Relative fluorescence values of the wild-type mBFP, mutant proteins, and BFPbc. All reactions were conducted in triplicate and their average values are described.

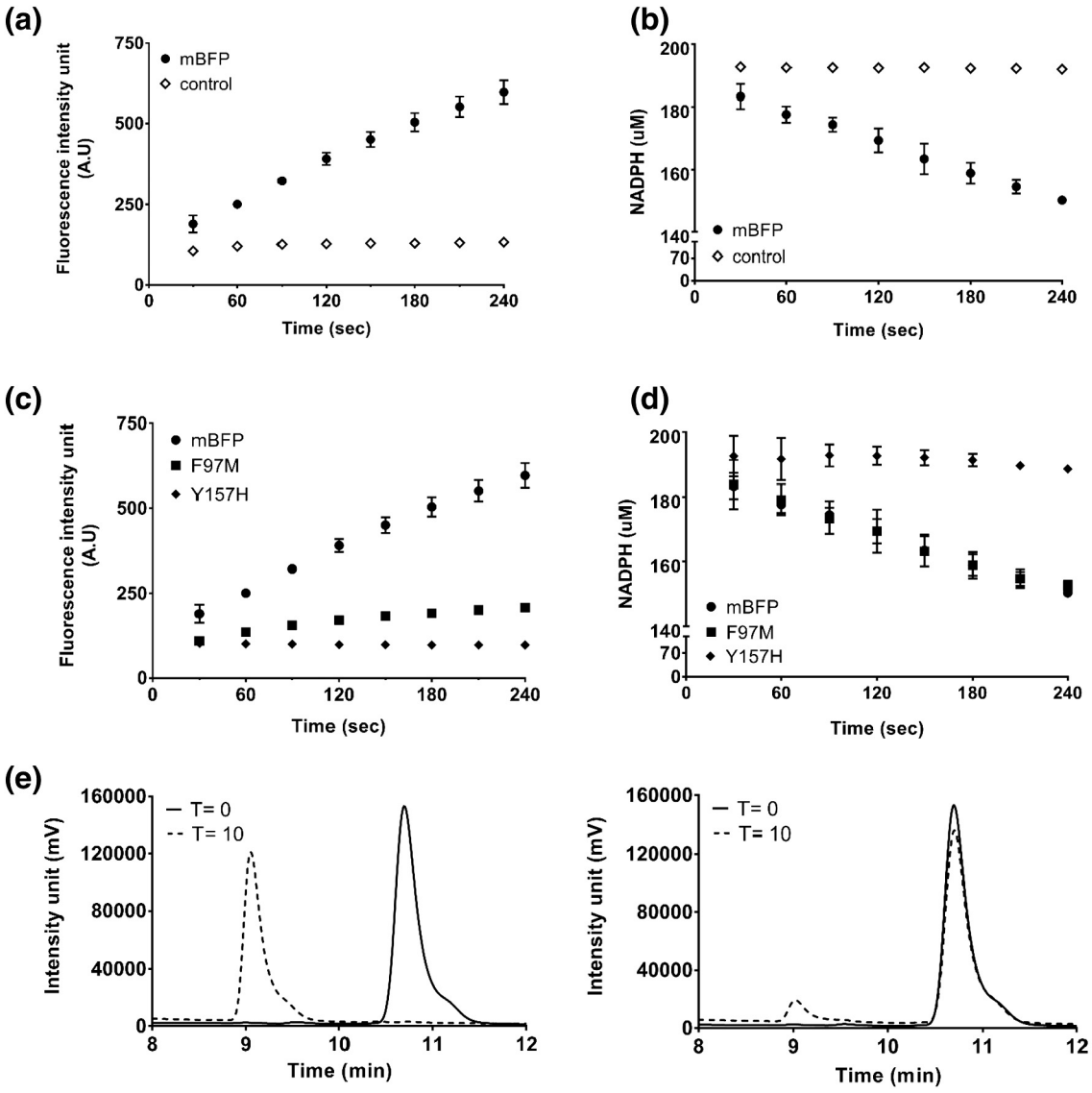

Fig. 4. Activity profiles of the wild-type mBFP and mutant proteins. Activity profiles of mBFP toward putative substrates acetaldehyde (a) and nitrobenzaldehyde (b). The reaction mixture consisted of mBFP, and a cofactor without each substrate was used as a control. (c) Comparison of activity profiles toward acetaldehyde between the wild-type and mutant enzymes. The oxidized reaction of mBFP was recorded by the increased fluorescence of NADPH using the reducing $NADP^+$ as a cofactor. (d) Activity profiles with nitrobenzaldehyde substrate. The enzymatic activity of mBFP was recorded by the abundance of NADPH as a cofactor. (e) Activity of mBFP toward nitrobenzaldehyde confirmed by HPLC. All reaction profiles were conducted in duplicate, and average values were plotted with respect to time.

Generation of an mBFP derivative with constant fluorescence

In our previous report, mBFP was tested as a potential reporter or quantitative tool due to its dose-dependent fluorescent capacity with NADPH [13]. Preliminary characterizations of mBFP using the linear relationship, standard deviation, and spiking-recovery assays strongly supported mBFP as a plausible quantitative reporter [13]. However, assays in the presence of putative substrates have demonstrated increased fluorescence with acetaldehyde, or a decreased absorbance of NADPH with nitrobenzaldehyde, in a time-dependent manner (Fig. 4). We arbitrarily monitored the amount of NADPH instead of its fluorescence in the assay with nitrobenzaldehyde substrate, due to the high background fluorescence of nitrobenzaldehyde under our assay conditions. In summary, the enzymatic property of mBFP as a dehydrogenase or reductase sets its limitation as a stable reporter system.

We further screened the constructed mutants for any derivative that exhibits constant fluorescence in the presence of a putative substrate, nitrobenzaldehyde or

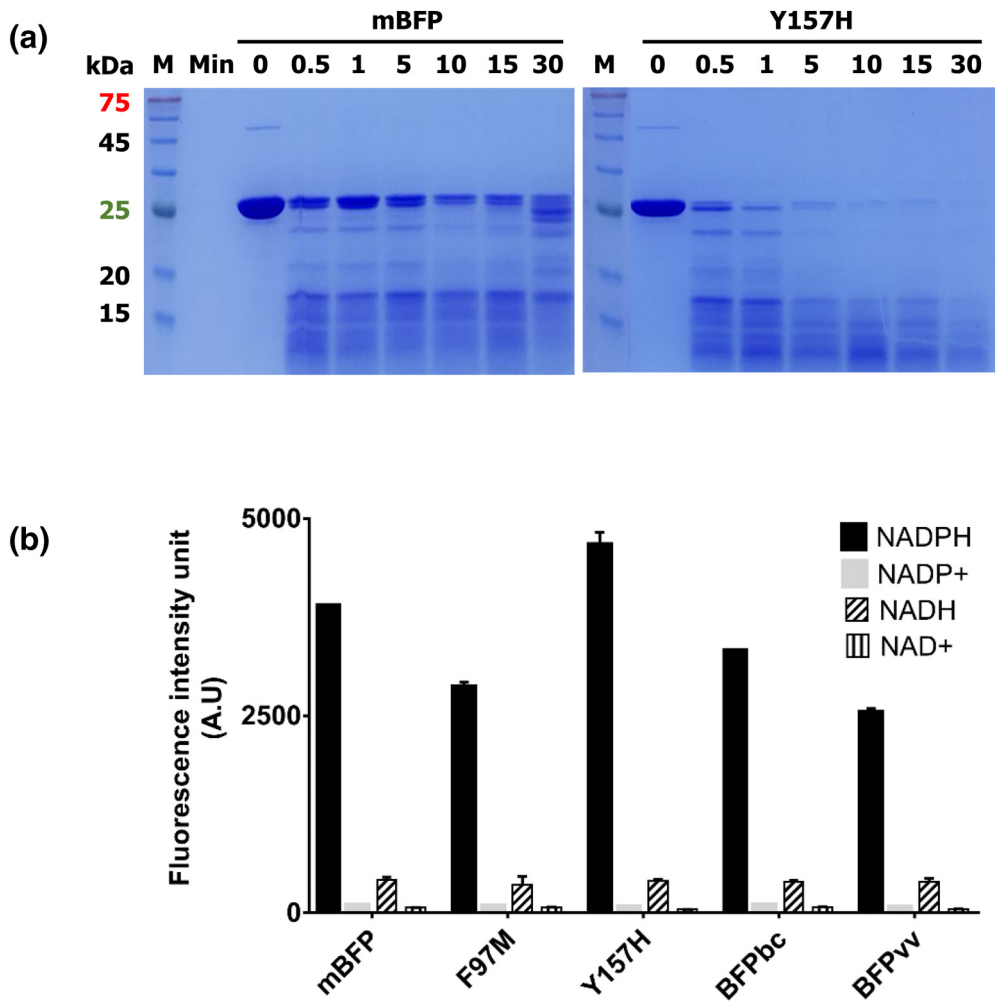

Fig. 5. Protease K susceptibility and cofactor specificity. (a) Comparison of digestion patterns with protease K between wild-type mBFP and the mutant protein Y157H. (b) Cofactor specificity of the mutant Y157H. Functionally related enzymes, two wild-type (BFPbc and BFPvv) and a mutant (F97 M) protein were also analyzed.

acetaldehyde, in a time-independent manner. The mBFP Y157H mutant, which has shown a higher fluorescence than the wild-type (Fig. 3), has demonstrated constant fluorescence and constant levels of NADPH during the measured time interval in the presence of an acetaldehyde and a nitrobenzaldehyde, respectively (Fig. 4c and d). In contrast, the assay with another mutant F97 M, which has comparable fluorescence with the wild-type protein, exhibited a decreased NADPH level in the presence of nitrobenzaldehyde, exhibiting a pattern similar to the wild-type mBFP. The fluorescence of other mBFP derivatives was similar to the wild-type protein in various assay conditions with altering concentrations of the substrate and enzyme, and even with another tested acetaldehyde substrate (data not shown). Analysis of reaction products using high-performance liquid chromatography (HPLC) has also supported the results obtained from the NADPH amount assay (Fig. 4e). The wild-type mBFP completely converted the 4-nitrobenzaldehyde substrate to 4-nitrobenzylalcohol product within 10 min. On the other hand, only a small amount of product ($\ll$2% of the wild-type protein) was detected when mBFP Y157H and 4-nitrobenzaldehyde were reacting in the presence of NADPH within the same time interval, indicating that the catalytic activity of this mutant is inexistent, or highly inefficient compared to the wild-type protein. We investigated whether this difference is related with its quaternary structure or structural changes. The SEC elution profile (see Supplementary Fig. 1a) indicated no quaternary structural change with the introduction of mutation at this site. The expression level (~25%–30% of total protein) and yield (~85%–100 mg/L) of purification of this mutant were also similar to those of the wild-type mBFP (Fig. 5a). Notably, this mutant had slightly different emission spectra of intrinsic fluorescence from the wild-type protein (λ_{max} of 314–320 nm, Supplementary Fig. 3), although the excitation and

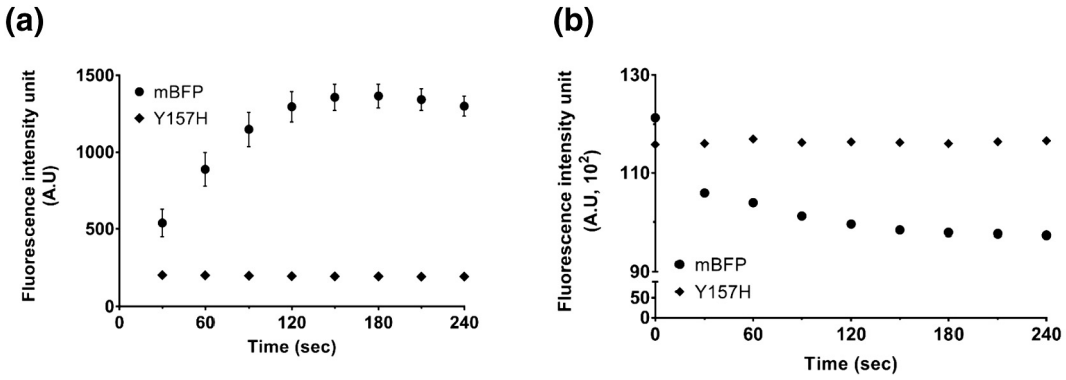

Fig. 6. Fluorescence in the presence of putative substrates with the crude cell extracts. The crude extract of *E. coil* cells was mixed with the purified enzymes and the putative substrate acetaldehyde (a) or nitrobenzaldehyde (b), and reaction profiles were monitored by the change in fluorescence.

emission wavelength of the fluorescence of protein/NADPH complex was identical to those of the wild-type mBFP. This mutant was, under *in vitro* conditions, more sensitive to protease K (Fig. 5a), which is specific for the peptide bond adjacent to the carboxyl group of aliphatic and aromatic amino acids [18]. The NADPH dependence of fluorescence of this mutant was also consistent (Fig. 5b), implying that mBFP derivatives without catalytic activity can be used as stable reporters *in vitro* as well as *in vivo*, regardless of intracellular metabolites [16,19].

This idea was further validated under the artificial reaction condition that mimics the cytoplasmic environment containing a putative substrate (nitrobenzaldehyde or acetaldehyde) and the corresponding cofactor NADPH or $NADP^+$. The crude extract of *E. coli* cells was mixed with acetaldehyde and $NADP^+$, and the reaction profile was monitored by measuring the fluorescence emitted by mBFP (Fig. 6a). While the fluorescence of wild-type mBFP increased and then decreased with time, the mBFP Y157H exhibited constant fluorescence. We also repeated the experiment with nitrobenzaldehyde as a substrate and NADPH as a cofactor (Fig. 6b), which resulted in a constant fluorescence after 60 s under our analytical condition. Intriguingly, the uniform profile was obtained when acetaldehyde was used as a substrate, strongly indicating that the mBFP Y157H derivative can be effectively utilized as a reporter protein *in vitro* as well as *in vivo*, upon consideration of the inevitable acetaldehyde-abundant environments in most cells. From this perspective, a previously well-known reporter system (iNap sensors) for NADPH-dependent fluorescence should also be functional in this condition and thus useful due to its specificity for the reduced cofactor NADPH and redox-independent function [20]. To the best of our knowledge, although further tuning and/or validation of *in vivo* function remain, the mutant protein with redox-independent function developed here would provide a basis to create a catalog of alternative NADPH sensing systems and supply the extended part for real time detection or imaging of the reduced cofactor NADPH *in vivo*.

Concluding Remarks

The fluorescent property of BFP proteins is closely related to the oxidation and reduction state of the NADPH cofactor embedded in the protein. All reported BFP proteins belong to SDR family, which is involved in oxidation or reduction of substrates by employing relevant cofactors. Hence, there is a high possibility that SDRs can catalyze cellular metabolites, implying that currently reported BFP proteins themselves cannot serve as stable reporters in living organisms that have various potential SDR substrates. The NADPH-dependent fluorescence of mBFP varies in a time-dependent manner with putative substrates, such as acetaldehyde and benzaldehyde. Interestingly, the mBFP Y157H derivative demonstrated time-independent fluorescence even in the presence of aldehyde substrates. Our results provide a fundamental basis for developing a reporting system that can be used regardless of the subcellular redox state and that is independent of the potential substrate.

Methods

Expression and purification of mBFP for structural studies

The metagenome-derived recombinant mBFP (GenBank No., ADG46021.1) and its mutant proteins were expressed in *E. coli* XL1-Blue strain (Stratagene, La Jolla, CA, USA) using the pQE30 expression vector with an N-terminal 6xHis tag

Table 2. The list of primers used for the saturation mutagenesis of F97 and Y157

Primer name	Sequences[a]
pQE30-Forward	ATTTCACACAGAATTCATTAAAGAGGAG
pQE30-Reverse	ATAAAGCTTTCAAGCGGCGAAGCCG
F97-Mutation R	GGCCGGCCAGMNNGATGCCGGCGT
F97-Mutation F	CGCCGGCATCNNKCTGGCCGGCC
Y157-Mutation R	TGCTGGCGGCMNNCAGCGTTAC
Y157H-Mutation F	GTAACGCTGNNKGCCGCCAGCA

Letter K indicates G or T sequence, and letter M indicates C or A sequence.
[a] The capital letter N indicates wobble sequences introduced in this position.

sequence. The recombinant cells were cultured in LB medium containing 100 µg/ml ampicillin at 37 °C without any inducer for 8 h under constant shaking (200 rpm), and then harvested by centrifugation at 6000 rpm for 10 min. The harvested cells were re-suspended and disrupted by ultrasonication in an ice-cold buffer (1× PBS) solution containing 20 mM imidazole, 135 mM NaCl, 2.7 mM KCl, 4.3 mM Na_2HPO_4, and 1.4 mM KH_2PO_4 (pH 7.4). The resulting supernatant was loaded onto a 1-mL Ni-NTA chelating column (GE Healthcare, Chicago, IL, USA), and the column was extensively washed with the same buffer containing 20 mM imidazole. The bound protein was eluted with a linear gradient from 0 to 500 mM of imidazole in the same buffer. When higher purity was required, the eluted protein from Ni-NTA column was further purified using a blue Sepharose column (GE Healthcare) with an affinity for nicotinamide cofactor binding protein [13] under the same conditions as above, with NaCl instead of imidazole.

Crystallization, data collection, and structure determination of mBFP

The purified recombinant mBFP protein was concentrated to 19 mg/ml in a buffer consisting of 20 mM Tris–HCl (pH 7.5) and 0.2 M NaCl. The protein concentration was determined considering the extinction coefficient of 0.293 M^{-1} cm^{-1} at 280 nm. The searching for the initial crystallizing condition was attempted at 294 K by the sitting-drop vapor-diffusion method using commercial screening kits and a 96-well crystallization plate (Corning, NY, USA). A drop composed of a mixture of 0.3 µl protein solution and 0.3 µl reagent was placed in each well of the sitting-drop plate and equilibrated with a 55 µl reservoir solution. The initial crystals were obtained from a precipitant solution consisting of 0.1 M Tris–HCl (pH 8.0), 0.3 M magnesium nitrate, 20% (w/v) PEG (polyethylene glycol) 2 K, and 2% (v/v) MPD (2-methyl-2,4-pentanediol). The initial condition was modified by changing the precipitant concentration, buffer pH, and the vapor-diffusion method to obtain suitable crystals for x-ray diffraction experiments. The optimized crystallization condition for proper diffraction data includes 0.1 M BICINE (2-(Bis(2-hydroxyethyl)amino)acetic acid) (pH 9.0), 0.3 M magnesium nitrate, 22% (w/v) PEG 2 K, and 4% MPD.

For x-ray diffraction experiments, crystals were immersed into the precipitant solution containing an additional 10% (v/v) ethylene glycol as a cryoprotectant for 5 s and immediately placed in a 100 K nitrogen-gas stream. The mBFP diffraction data set was collected at the wavelength of 0.9794 Å on the Beamline 11C of the Pohang Accelerator Laboratory (PAL) in Korea using a Pilatus 6 M detector (Dectris, Switzerland) [21] with an oscillation of 1 ° per frame, an exposure of 1 s per frame and a crystal-to-detector distance of 350 mm. The indexing, integration, and scaling of the reflections of the mBFP were conducted using the HKL2000 suite [22]. To get the NADPH-bound structure, the crystals were soaked for 90 min in a precipitation solution containing 6.7 mM NADPH. Diffraction data were also collected at the wavelength of 0.9793 Å on the Beamline 11C of PAL with an oscillation of 1 ° per frame, an exposure of 1 s per frame and a crystal-to-detector distance of 450 mm. The phase problem was solved by the AutoMR program of the PHENIX suite [23] using *S. meliloti* dehydrogenase reductase (PDB ID 3V2G) as a search model. Further model building and subsequent refinement were performed using WinCoot [24] and PHENIX [23], respectively. The data and refinement statistics are summarized in Table 1.

Construction, screening, and sequence analyses of saturation mutagenesis library for F97 and Y157 residues

In order to randomly cause mutations at the residue F97 and Y157 of mBFP, saturation mutagenesis was conducted by overlapping PCR using specifically designed wobble primers described in Table 2. Briefly, each N-terminal fragment of F97 and Y157 mutants were amplified by PCR using a set of primers, F97NF and F97NR, Y157NF, and Y157NR, respectively, according to the general protocol. C-terminal fragments of both mutants were also amplified by PCR using a set of primers, F97CF and F97CR, Y157CF, and Y157CR, respectively. The resulting fragments were amplified by PCR under the following conditions: preliminary denaturation at 92 °C for 5 min, then denaturation at 92 °C for 1 min, annealing at 52 °C for 1 min, and extension at 72 °C for 1 min. After 30 cycles of PCR amplifications, the overlapping DNA fragments were eluted from agarose gel (0.8%) by using a DNA clean-up system (Zymo Research, Irvine, CA, USA) and digested with two restriction enzymes, EcoRI

and HindIII. The resulting genes were cloned into the same sites on pQE30 with N-terminal His-tag and transformed into *E. coli* XL1-Blue. The recombinant cells were spread onto solid LB media containing 100 μg/ml ampicillin and further grown at 37 °C overnight without any inducer. The primary screening of candidate clones emitting different levels of blue fluorescence was conducted by excitation with a wavelength of 395 nm using a UV-ramp and further confirmed by re-seeding in liquid LB media under the same conditions by using a spectrofluorometer (Infinite-200; Tecan, Männedorf, Switzerland). As a control, the clone harboring the wild-type mBFP was grown under the same conditions. For the sequence analyses of mutated genes, the recombinant plasmids were isolated from screened clones with high, low, and merely detectable fluorescence. We prepared three independent mutagenesis libraries, according to the procedure above, and finally screened 10 (F97A, F97D, F97E, F97G, F97H, F97K, F97M, F97N, F97S, and F97Y) and 9 (Y157D, Y157E, Y157G, Y157H, Y157L, Y157N, Y157S, Y157V, and Y157W) mutants from the saturation mutagenesis library of F97 and Y157 residues of mBFP, respectively.

Purification and gel-filtration of mutant proteins

The purification of mutant proteins was attempted according to the same procedure as with the wild-type protein described above. When required, the desalting was conducted by using the column Sephadex G-10 (GE Healthcare). The protein homogeneity and concentration were determined using a 10% SDS-PAGE and a dye-binding method (Bio-Rad, Hercules, CA, USA), respectively.

The quaternary structure of the mutant proteins was analyzed using gel filtration chromatography (Superose TM12; GE Healthcare). The purified protein (2.5 μM) was placed in 1× PBS buffer (pH 7.4) and monitored at a flow rate of 0.5 ml/min. The calibration size marker protein (Sigma, St. Louis, MO, USA) and the wild-type protein mBFP were used as controls.

Intrinsic fluorescence, cofactor specificity, and enzyme assays

The intrinsic fluorescence and cofactor specificity of mutant proteins were determined using a purified protein (5 μM) and spectrofluorometer (Infinite-200; Tecan) under the defined conditions (25 °C, PBS, pH 7.4). The intrinsic fluorescence of mutant proteins was recorded by scanning of the emission wavelength from 250 to 500 nm under the excitation of 280 nm. The cofactor specificity of mutant proteins was determined by relative fluorescence at the emission wavelength of 450 nm (excitation wavelength of 350 nm) after mixing with oxidized (NAD^+ and $NADP^+$) and reduced (NADH and NADPH) cofactors (20 μM) under the condition defined above. As controls, the level of intrinsic and NADPH-dependent fluorescence of the wild-type protein mBFP was analyzed under the same conditions as the mutant proteins.

The activities of mutant proteins from the pool of the saturation mutagenesis library were determined at 25 °C for 1–5 min by a spectrofluorometer using the microplate reader format. The amounts of substrate and cofactors used were determined by using either a spectrophotometer at an absorbance wavelength of 365 nm or a spectrofluorometer. The enzyme reaction was carried out with the purified enzyme (0.1–5 μM) in 0.1 ml of reaction mixture (1× PBS, pH 7.4) containing 0.3 mM NADPH and 0.3–0.5 mM nitrobenzaldehyde (or acetaldehyde). As quantitative controls, a decrease in the concentration of nitrobenzaldehyde substrate and an increase in the production of the corresponding nitrobenzyl alcohol were also analyzed by HPLC according to the typical procedure reported in a previous report [16]. All assays were carried out in triplicate. One unit of enzyme activity was defined as the amount of enzyme required to convert 1 μmol of the substrate benzaldehyde per minute under the specified conditions.

Protease K sensitivity and reaction profile in crude extracts with putative substrates

The resistance to the digestion with protease K was validated in a solution containing the purified protein (5.05 μg) and protease K (0.0159 mAU; Gold Bio, St. Louis, MO, USA) at 25 °C for 1–30 min. After incubation at indicated time interval, each reaction solution was mixed with sample buffer, and analyzed with a 12% SDS-PAGE gel.

To compare the reaction profile of mBFP with the mutant Y157H in crude cell extracts, 100 ml of the cultured *E. coli* XL1-blue cells (OD = 2.0) was harvested and suspended in a 20 ml of buffer (1× PBS, pH 7.4). Cells were disrupted by sonication and the supernatant was separated by centrifugation at 6000 rpm for 10 min. An aliquot (20–80 μl) of crude cell extracts was added into a 0.1 ml reaction solution containing 1× PBS buffer (pH 7.4), 0.3–0.6 mM NADP (H), and 0.2–1 mM putative substrate. During the incubation of the reaction mixture for 6 min, mBFP-mediated fluorescence was measured by the microplate reader. When required to adjust the background signal to be similar between the wild-type and mutant protein, the disrupted cells were desalted by using a dialysis tube (SnakeSkin™; Thermo Fisher Scientific) to remove intracellular cofactors and metabolites.

Accession numbers

Coordinates and structure factors have been deposited in the Protein Data Bank with accession numbers 6J7H and 6J7U.

Acknowledgments

The x-ray diffraction experiments were performed with Beamline 11C at the Pohang Accelerator in Korea. This work was supported by Basic Science Research programs [NRF Grant Number: 2017R1D1A3B03032278 (to J.-S.K), 2017R1D1A1B03034080 and 2018R1A4A1023882 (to G.-J.K)] of the National Research Foundation (NRF) of Korea funded by the Ministry of Education, Science and Technology of Korea. This work was also supported by the Intelligent Synthetic Biology Center [NRF-2017030616 (to G.-J.K)] program of NRF funded by the Ministry of Science, ICT & Future Planning and supported by a grant from Marine Biotechnology Program [20170305 (to G.-J.K)] funded by Ministry of Oceans and Fisheries, Korea.

Competing Interest: All authors declare no competing interests.

Appendix A. Supplementary data

Supplementary data to this article can be found online at https://doi.org/10.1016/j.jmb.2019.06.005.

Received 13 February 2019;
Received in revised form 30 April 2019;
Available online 13 June 2019

Keywords:
fluorescent proteins;
mBFP;
redox;
short-chain dehydrogenase/reductase

These two authors contributed equally to this work.

Abbreviations used:

GFP, green fluorescent protein; BFP, blue fluorescent protein; mBFP, BFP from soil metagenomes; SDR, short-chain dehydrogenase/reductase; BFPvv, BFP from *Vibrio vulnificus*; BFPbc, from *Burkholderia cenocepacia* J2315.

References

[1] A. Ettinger, T. Wittmann, Fluorescence live cell imaging, Methods Cell Biol. 123 (2014) 77–94.
[2] S. Okumoto, A. Jones, W.B. Frommer, Quantitiative imaging with fluorescent bioseonsors, Annu. Rev. Plant Biol. 63 (2012) 663–706.
[3] C.H. Contag, M.H. Bachmann, Advances in vivo bioluminescence imaging of gene expression, Annu. Rev. Biomed. Eng. 4 (2002) 235–260.
[4] R.Y. Tsien, The green fluorescent protein, Annu. Rev. Biochem. 67 (1998) 509–544.
[5] Q. Ni, S. Mehta, J. Zhang, Live-cell imaging of cell signaling using genetically encoded fluorescent reporters, FEBS J. 285 (2018) 203–219.
[6] S.J. Remington, Fluorescent proteins: maturation, photochemistry and photophysics, Curr. Opin. Struct. Biol. 16 (2006) 714–721.
[7] T.D. Craggs, Green fluorescent protein: structure, folding and chromophore maturation, Chem. Soc. Rev. 38 (2009) 2865–2875.
[8] T. Drepper, T. Eggert, F. Circolone, A. Heck, U. Krauss, J.K. Guterl, M. Wendorff, A. Losi, W. Gärtner, K.E. Jaeger, Reporter proteins for in vivo fluorescence without oxygen, Nat. Biotechnol. 25 (2007) 443–445.
[9] X. Shu, A. Royant, M.Z. Lin, T.A. Aguilera, V. Lev-Ram, P.A. Steinbach, R.Y. Tsien, Mammalian expression of infrared fluorescent proteins engineered from a bacterial phytochrome, Science 324 (2009) 804–807.
[10] A. Kumagai, R. Ando, H. Miyatake, P. Greimel, T. Kobayashi, Y. Hirabayashi, T. Shimogori, A. Miyawaki, A bilirubin-inducible fluorescent protein from eel muscle, Cell 153 (2013) 1602–1611.
[11] A. Mukherjee, J. Walker, K.B. Weyant, C.M. Schroeder, Characterization of flavin-based fluorescent proteins: an emerging class of fluorescent reporters, PLoS One 8 (2013) 15.
[12] J. Herrou, S. Crosson, Function, structure and mechanism of bacterial photosensory LOV proteins, Nat. Rev. Microbiol. 9 (2011) 713–723.
[13] C.S. Hwang, E.S. Choi, S.S. Han, G.J. Kim, Screening of a highly soluble and oxygen-independent blue fluorescent protein from metagenome, Biochem. Biophy. Res. Commun. 419 (2012) 676–681.
[14] T.H. Kao, Y. Chen, C.H. Pai, M.C. Chang, A.H.J. Wang, Structure of a NADPH-dependent blue fluorescent protein revealed the unique role of Gly176 on the fluorescence enhancement, J. Struct. Biol. 174 (2011) 485–493.
[15] T. Drepper, R. Huber, A. Heck, F. Circolone, A.K. Hillmer, J. Büchs, K.E. Jaeger, Flavin mononucleotide-based fluorescent reporter proteins outperform green fluorescent protein-like proteins as quantitative in vivo real-time reporters, Appl. Environ. Microb. 76 (2010) 5990–5994.
[16] K.M. Polizzi, D.A. Moore, A.S. Bommarius, A short-chain dehydrogenase/reductase from *Vibrio vulnificus* with both blue fluorescence and oxidoreductase activity, Chem. Commun. (18) (2007) 1843–1845.
[17] S.H. You, H.D. Lim, D.E. Cheong, E.S. Kim, G.J. Kim, Rapid and sensitive detection of NADPH via mBFP-mediated enhancement of its fluorescence, PLoS One 14 (2019), e0212061.
[18] W. Ebeling, N. Hennrich, M. Klockow, H. Metz, H.D. Orth, H. Lang, Proteinase K from *Tritirachium album* limber, Eur. J. Biochem. 47 (1974) 91–97.
[19] O. Goldbeck, A.W. Eck, G.M. Seibold, Real time monitoring of NADPH concentrations in *Corynebacterium glutamicum* and *Escherichia coli* via the genetically encoded sensor mBFP, Front. Microbiol. 9 (2018) 2564.
[20] R. Tao, Y. Zhao, H. Chu, A. Wang, J. Zhu, X. Chen, Y. Zou, M. Shi, R. Liu, N. Su, J. Du, H.M. Zhou, L. Zhu, X. Qian, H. Liu, J. Loscalzo, Y. Yang, Genetically encoded fluorescent sensors reveal dynamic regulation of NADPH metabolism, Nat Methods 14 (2017) 720–728.
[21] S.Y. Park, S.C. Ha, Y.G. Kim, The protein crystallography beamlines at the pohang light source II, Biodesign 5 (2017) 30–34.

[22] Z. Otwinowski, W. Minor, Processing of x-ray diffraction data collected in oscillation mode, Methods Enzymol. 276 (1997) 307–326.
[23] P.D. Adams, P.V. Afonine, G. Bunkóczi, V.B. Chen, I.W. Davis, N. Echols, J.J. Headd, L.W. Hung, G.J. Kapral, R.W. Grosse-Kunstleve, A.J. McCoy, N.W. Moriarty, R. Oeffner, R. J. Read, D.C. Richardson, J.S. Richardson, T.C. Terwilliger, P.H. Zwart, PHENIX: a comprehensive python-based system for macromolecular structure solution, Acta Crystallogr. D Struct. Biol. 66 (2010) 213–221.
[24] P. Emsley, K. Cowtan, Coot: model-building tools for molecular graphics, Acta crystallogr. D Biol. Crystallogr. 60 (2004) 2126–2132.